

# **Influence of small scale heterogeneity on CO<sub>2</sub> trapping processes in deep saline aquifers**

**Naum I. Gershenzon, Mohamad Reza Soltanian, Robert W. Ritzi Jr.,  
David F. Dominic**

Department of Earth and Environmental Sciences, Wright State University, 3640 Col.  
Glenn Hwy., Dayton, OH 45435

Naum I. Gershenzon ([naum.gershenzon@wright.edu](mailto:naum.gershenzon@wright.edu))

## **ABSTRACT**

The physical mechanism of CO<sub>2</sub> trapping in porous media by capillary trapping (pore scale) incorporates a number of related processes, i.e. residual trapping, trapping due to hysteresis of the relative permeability, and trapping due to hysteresis of the capillary pressure. Additionally CO<sub>2</sub> may be trapped in heterogeneous media due to difference in capillary pressure entry points for different materials (facies scale). The amount of CO<sub>2</sub> trapped by these processes depends upon a complex system of non-linear and hysteretic relationships including how relative permeability and capillary pressure vary with brine and CO<sub>2</sub> saturation, and upon the spatial variation in these relationships as caused by geologic heterogeneity.

Geological heterogeneities affect the dynamics of CO<sub>2</sub> plumes in subsurface environments. Recent studies have led to new conceptual and quantitative models for sedimentary architecture in fluvial deposits over a range of scales that are relevant to the performance of some deep saline reservoirs. We investigated how the dynamics of a CO<sub>2</sub> plume, during and after injection, is influenced by the hierarchical and multi-scale stratal architecture in such reservoirs. The results strongly suggest that representing small scales features (decimeter to meter), including their organization within a hierarchy of larger-scale features, is critical to understanding trapping processes.

## 1. INTRODUCTION

The idea of sequestering CO<sub>2</sub> in the Earth's crust has been discussed and evaluated for more than two decades (e.g. Steinberg, 1992; Hitchon et al., 1999; Bachu, 2000). The most likely sites for sequestration are deep saline aquifers and depleted hydrocarbon reservoirs (Holloway, 2001; Kovscek and Wang, 2005; Kovscek and Cakici, 2005, Bruant et al., 2002; Pruess and Garcí'a, 2002; Bachu, 2003; Deng et al., 2012; Dai et al., 2013). Sites must be evaluated for reservoir capacity and the risk of CO<sub>2</sub> leakage, which requires detailed modelling of CO<sub>2</sub> movement. Such modeling must account for coupled processes occurring over a wide range of scales. For example Middleton et al. (2012) defined and described processes relevant at these scales: sub-pore (Å -10 nm), pore (10 nm- 10 cm), CO<sub>2</sub> reservoir (10 cm – 100 m), site (100 m – 10 km, the deep groundwater system), and region (10 km – 1 Mm, the sedimentary basin). At any site dependent on structural (or hydrodynamic) trapping, caprock may be compromised by improperly abandoned wells, stratigraphic discontinuities, or faults. Therefore, other trapping mechanisms must be considered, including, dissolution, mineralization, and capillary trapping. We focus on capillary trapping processes that operate over a range of scales of heterogeneity intermediate between the pore scale (c.f. Kuo and Benson, 2013) and the site scale (c.f. Zhou et al., 2009), scales that have not yet received full consideration in the literature.

Typically, CO<sub>2</sub> is injected in a supercritical state with liquid-like properties. After injection the CO<sub>2</sub> plume migrates towards the top of the reservoir, driven by buoyancy forces. CO<sub>2</sub> becomes virtually immobile due either to capillary trapping in reservoir rock pores (time scale: 10 to 100 years), dissolution of CO<sub>2</sub> into brine (100 to 1000 years), or mineral trapping through reaction with rock minerals (thousands to millions of years) (Xu et al., 2003; IPCC, 2007; and Hesse et al., 2007). We modelled both capillary trapping and dissolution processes, but our main interest is in capillary trapping, especially the effects of reservoir heterogeneity.

Geological heterogeneities affect the dynamics of CO<sub>2</sub> plumes in subsurface environments. Their role in capillary trapping and dissolution of CO<sub>2</sub> has been investigated extensively (Hovorka et al., 2004; Doughty and Pruess, 2004; Kumar et al.,

2005; Bryant et al., 2006; Forster et al., 2006; Ambrose et al., 2008; Ide et al., 2007; Flett et al., 2007; Tsang et al., 2008; Han et al., 2010; Sakaki et al., 2013). Usually the effects of heterogeneity are considered within two-dimensional geostatistical models using various correlation lengths. While such an approach is capable of capturing qualitatively some typical features of the process, full understanding requires modeling three-dimensional flow within reservoirs with realistic representations of sedimentary architecture and the associated relative permeability and capillary pressure distributions, across a range of scales.

Recent studies have led to new conceptual and quantitative models for sedimentary architecture in fluvial deposits over a range of scales that are relevant to fluid flow in some petroleum and deep saline reservoirs (e.g. Lunt et al., 2004; Bridge, 2006; Lunt and Bridge 2007). From these studies emerged a generalized, three-dimensional, quantitative model for the multiscale and hierarchical stratal architecture found in fluvial deposits. Importantly, the lengths of stratal units at all hierarchical levels scale together with the width of the formative channels (Bridge, 2006), making it possible to adapt the general model to specific deposits. The software package (GEOSIM) uses a geometric-based approach to create three-dimensional geocellular models representing this multiscale and hierarchical fluvial architecture (Ramanathan et al., 2010; Guin et al. 2010; Ritzi, 2013).

Here we focus on fluvial deposits dominated by sandy gravel. Lunt et al. (2004) studied the gravelly channel belt of the Sagavanirktok River Alaska, an analog for a number of important reservoirs composed of fluvial deposits (e.g. Tye et al., 2003, Zhou et al., 2009). At the smallest scale are sets of cross-strata (decimeters thick and meters long), which occur within unit bar deposits (tens of decimeters thick and tens of meters long). Unit bars and cross-bar channel fills occur within compound bar deposits (meters thick and hundreds of meters long). Compound bar deposits and the channel fills that bound them occur within channel belts (tens of meters thick and kilometers long). Importantly, open-framework gravel (OFG) cross strata are known to create preferential flow pathways that confound attempts at gas injection (e.g. Tye et al., 2003). The OFG are found to make up 25 to 30 percent of the volume of a deposit.

The complexity of the heterogeneity and highly non-linear nature of the problem make it challenging to achieve numerically convergent solutions. Consequently, the

simulations presented here are limited to an examination of CO<sub>2</sub> within a relatively small reservoir compartment of 100 m x 100 m x 5 m (illustrated in Gershenson et al., 2014). Our longer-term goal is to run larger simulations that include more of the geocellular model (e.g. Ramanathan et al., 2010, Figure 10), and thus include some of the larger-scale sedimentary architecture not yet represented here. However, the preliminary work presented here shows the fundamental importance of properly representing the within-reservoir heterogeneity, and therefore justifies this line of research.

In the following sections we review background research (Section 2), give short overview of fluvial reservoir model (Section 3), describe the simulations framework of CO<sub>2</sub> sequestration in saline aquifer (Section 4) and finally present and discuss the results of simulation (Section 4).

## **2. BACKGROUND**

Here we will focus our attention mainly on processes at the reservoir scale. The main short-term (~10 years) physical mechanism of CO<sub>2</sub> trapping in porous media is capillary trapping (this term incorporates three related mechanisms, i.e. residual trapping, trapping due to hysteresis of the relative permeability, and trapping due to hysteresis of the capillary pressure) (Kumar et al., 2005; Mo et al., 2005; Spiteri et al., 2008; Juanes et al., 2006; Altundas et al., 2011). The basics of this mechanism are as follow. After injection into deep saline aquifers, the low viscosity CO<sub>2</sub> tends to migrate to the top of the geologic structure due to a density difference between the CO<sub>2</sub> and the brine. During the injection period CO<sub>2</sub> displaces brine in a drainage process. After the injection is finished, the buoyant CO<sub>2</sub> migrates upward and water displaces CO<sub>2</sub> at the plume “tail” in an imbibition-like process. The latter causes CO<sub>2</sub> stream disconnection into immobile blobs and ganglia (Hunt et al., 1988). The amount of CO<sub>2</sub> trapped by this mechanism is a complicated nonlinear function of the spatial distribution of permeability, permeability anisotropy, capillary pressure, relative permeability of brine and CO<sub>2</sub>, permeability hysteresis and residual gas saturation, as well as the rate, total amount and placement of injected CO<sub>2</sub>. Kumar et al. (2005), analyzing residual and aqueous CO<sub>2</sub> trapping, showed that the former is a dominant short-term trapping mechanism. Aquifer dip and

permeability anisotropy have an effect on gas migration and hence affects CO<sub>2</sub> dissolution in brine. Juanes et al. (2006) found that relative permeability hysteresis becomes a major factor in CO<sub>2</sub> trapping. High injection rates and injection of water slugs alternating with CO<sub>2</sub> injection increases the effectiveness of the sequestration project. They also observed that coarse simulation models overestimate capillary trapping of CO<sub>2</sub>, suggesting high-resolution models for accurate assessment of the different storage mechanisms. Ide et al. (2007) established that the amount of CO<sub>2</sub> immobilized by residual trapping is a strong function of the gravity number (the ratio between viscous and gravitational forces (Zhou et al. 1994)). Altundas et al. (2011) showed that not only hysteresis of permeability but also hysteresis of capillary pressure affects the dynamics of CO<sub>2</sub> trapping. The latter mechanism works not only on the tail of the CO<sub>2</sub> plume but at the front as well, causing its retardation.

The solubility trapping is also an important and safe CO<sub>2</sub> storage mechanism (Pruess and Garcí'a, 2002; Ennis-King and Paterson, 2005). CO<sub>2</sub> dissolution is a slow diffusion process. The rate of CO<sub>2</sub> dissolution in brine depends on the contact area between these two phases. Since the CO<sub>2</sub>-brine solution has a density greater than brine alone, convective motion is initiated under appropriate conditions (Lindeberg and Wessel-Berg, 1997). If convection does develop, the contact area considerably increases, and this mechanism may become a dominant form of CO<sub>2</sub> storage in aquifers over periods of tens to hundreds of years.

Numerous studies have considered the influence of different types of heterogeneity on reservoir performance of CO<sub>2</sub> sequestration in saline formations. Hovorka et al. (2004), modeling a CO<sub>2</sub> injection test in the Frio Formation of the upper Texas Gulf Coast, concluded that stratigraphic heterogeneity may result in significant channeling of the flow of a CO<sub>2</sub> plume. Doughty and Pruess (2004) created three-dimensional models representing the fluvial/deltaic Frio Formations in the upper Texas gulf coast. Their simulations also demonstrate the strong influence of geologic heterogeneity on buoyancy-driven CO<sub>2</sub> migration. Obi and Blunt (2006), considering the lateral movement (advection) of the CO<sub>2</sub> plume under a horizontal pressure gradient, found that permeability heterogeneity causes the CO<sub>2</sub> to migrate much further than predicted from a homogeneous model. This allows trapping mechanisms to be more efficient than in the

homogeneous case, leading to significant impedance of the movement of CO<sub>2</sub>. However the sequestration efficiency of reservoir is considerably less than in the homogeneous case. Ide et al. (2007) studied CO<sub>2</sub> plume dynamics in two-dimensional layered reservoirs. The permeability maps for the various layers were created using a geo-statistical model. The influences of different correlation coefficients on the permeability distribution were analyzed. It was shown that the difference is small in the gas distribution between the homogeneous case and the cases of heterogeneity with short and long permeability correlation. Bryant et al. (2006) investigated the instability of the CO<sub>2</sub>-brine interface in heterogeneous two-dimensional reservoirs. They observed the formation of narrow closely-spaced CO<sub>2</sub> channels. The placement of these channels is correlated with permeability channels, suggesting that the preferential-flow paths of buoyancy-driven CO<sub>2</sub> displacement are due to heterogeneity of the aquifer rather than fingering due to viscous instability. The rising CO<sub>2</sub> front is smoothed if capillary pressure is included in the simulation, since capillary and buoyancy forces are of similar magnitude. Bryant et al. (2006) and Ide et al. (2007) showed that a layer of smaller permeability lying above a layer of larger permeability can act as a seal due to capillary pressure barrier. Saadatpoor et al. (2009) further exposed this additional trapping mechanism, which they termed a “local trapping mechanism.” Supposing a functional dependence between permeability and capillary pressure, they simulated the dynamics of the buoyant CO<sub>2</sub>-brine front in a heterogeneous reservoir. Comparison of this simulation with an analogous simulation but with a homogeneous (averaged) capillary pressure curve revealed a dramatic difference in results. In the former case CO<sub>2</sub> rises through the high permeability channels, which are surrounded by the capillary barriers of the low permeability material. In some regions capillary barriers prevent upward movement of CO<sub>2</sub>, allowing only lateral migration, which effectively traps the CO<sub>2</sub> plume. The same idea has been exploited by Zhou et al. (2009). Considering a regional-scale (typical lateral size up to a few km) flow and transport processes in a layered reservoir, they investigated the “secondary-seal effect”, i.e. the effect of CO<sub>2</sub> accumulation between layers with different permeability and capillary pressure entry points, causing retardation of upward CO<sub>2</sub> migration. Flett et al. (2007), using standard geo-statistical techniques, generated various three-dimensional reservoir realizations with different sand-to-shale

proportions. They found that the increase of shale content reduces the rate of residual CO<sub>2</sub> trapping. Han et al. (2010) systematically investigated the influence of heterogeneity in the permeability distribution (generated by geo-statistical techniques in two-dimensional reservoirs) on CO<sub>2</sub> trapping mechanisms and buoyancy-driven CO<sub>2</sub> migration. They found that 1) the amount of residually trapped CO<sub>2</sub> is enhanced if CO<sub>2</sub> plume migrates farther in the vertical or lateral direction; 2) the presence of low permeability inclusions (secondary caprock) enhances residual CO<sub>2</sub> trapping; 3) increasing the degree of permeability heterogeneity decreases the amount of residual CO<sub>2</sub> trapping.

Simulations at the reservoir scale critically depend on relative permeability and capillary pressure curves for drainage and imbibition (e.g. Doughty and Pruess, 2004; Kumar et al., 2005; Mo and Akervoll, 2005; Juanes et al., 2006; Burton et al 2009; Altundas et al., 2011). These parameters are difficult to measure and are quite uncertain for most potential reservoirs. Various approaches have been used to determine interconnection between petrophysical parameters and to specify the Brooks-Corey relations for capillary pressure and relative permeability curves (Holtz, 2002; Altundas et al., 2011; Delshad et al., 2013). To define irreducible water saturation and residual CO<sub>2</sub> saturation, Holtz (2002) uses empirical relations between these parameters and porosity, and the latter is defined from the empirical relation between permeability and porosity. Altundas et al. (2011) modified the Brooks-Corey relation for imbibition by redefining the normalization of relative saturation and introducing a coefficient to characterize the pore-body radius to pore-throat radius ratio. Delshad et al. (2013) have proposed a method that uses the relations between petrophysical parameters and interfacial tension to define the permeability and capillary pressure. Krevor et al. (2012) measured capillary pressure and relative permeability for four different sandstone rocks including Mt. Simon and Berea formations (the potential sites for CO<sub>2</sub> injection). They provide the best-fit Brooks-Corey parameters for both capillary pressure and relative permeability curves for CO<sub>2</sub>.

Different storage strategies have been proposed to reduce the amount of mobile CO<sub>2</sub> and to increase the capacity of reservoir. The “inject low and let rise” strategy is the obvious one (the larger distance between an injection point and a caprock the more CO<sub>2</sub>

will be trapped by capillary trapping) (Kumar et al, 2005). Juanes et al. (2006) showed that high injection rates and a shorter injection period as well as injection of a water slug alternating with CO<sub>2</sub> injection result in more effective sequestration. The simulation results by Ide et al. (2007) suggest that the amount of trapping can be maximized by injecting CO<sub>2</sub> at the lowest feasible value of the gravity number, which can be controlled by adjusting the injection rate. Leonenko and Keith (2008) proposed injecting brine after CO<sub>2</sub> to dissolve all of injected CO<sub>2</sub> in a shorter time. The downside of this strategy is a severe limitation of storage capacity of an aquifer. Qi et al. (2009) demonstrated that simultaneously injected CO<sub>2</sub> and formation brine followed by chase brine mitigates the mobility contrast between injected and displaced fluids, leading to higher storage efficiencies than injecting CO<sub>2</sub> alone. Shamshiri and Jafarpour (2012), based on simulations in heterogeneous reservoirs and counting CO<sub>2</sub> capillary trapping and solution in brine, proposed optimization algorithms to improve the CO<sub>2</sub> storage efficiency.

### **3. OVERVIEW OF THE GEOLOGIC MODEL**

The complexity and uncertainty of stratal architecture of saline aquifers and hydrocarbon reservoirs make it difficult to predict the actual behavior of a CO<sub>2</sub> plume and to evaluate the reservoir capacity and the risk of CO<sub>2</sub> leakage. Many sites suitable for CO<sub>2</sub> sequestration have fluvial-type architecture, i.e. structure with multi-scale heterogeneities ranging from the centimeter to the reservoir scale.

The sedimentary architecture of reservoirs created by fluvial deposition has recently been described in three-dimensional models (Bridge, 2006). As shown in Figure 1, channel-belt deposits are characterized by a large volume fraction of convex-up, bar deposits formed within channels. Only when channels are abandoned and filled under lower flows are “channel-shaped” units formed. These concave-up channel fills are low-permeability baffles within the domain. In gravelly channel-belt deposits, preferential flow pathways arise from the interconnection of open-framework gravels within lobate unit bar deposits (Lunt and Bridge, 2007). These are the “thief zones” known by their negative effect on oil recovery (McGuire et al., 1999; Tye et al., 2003).

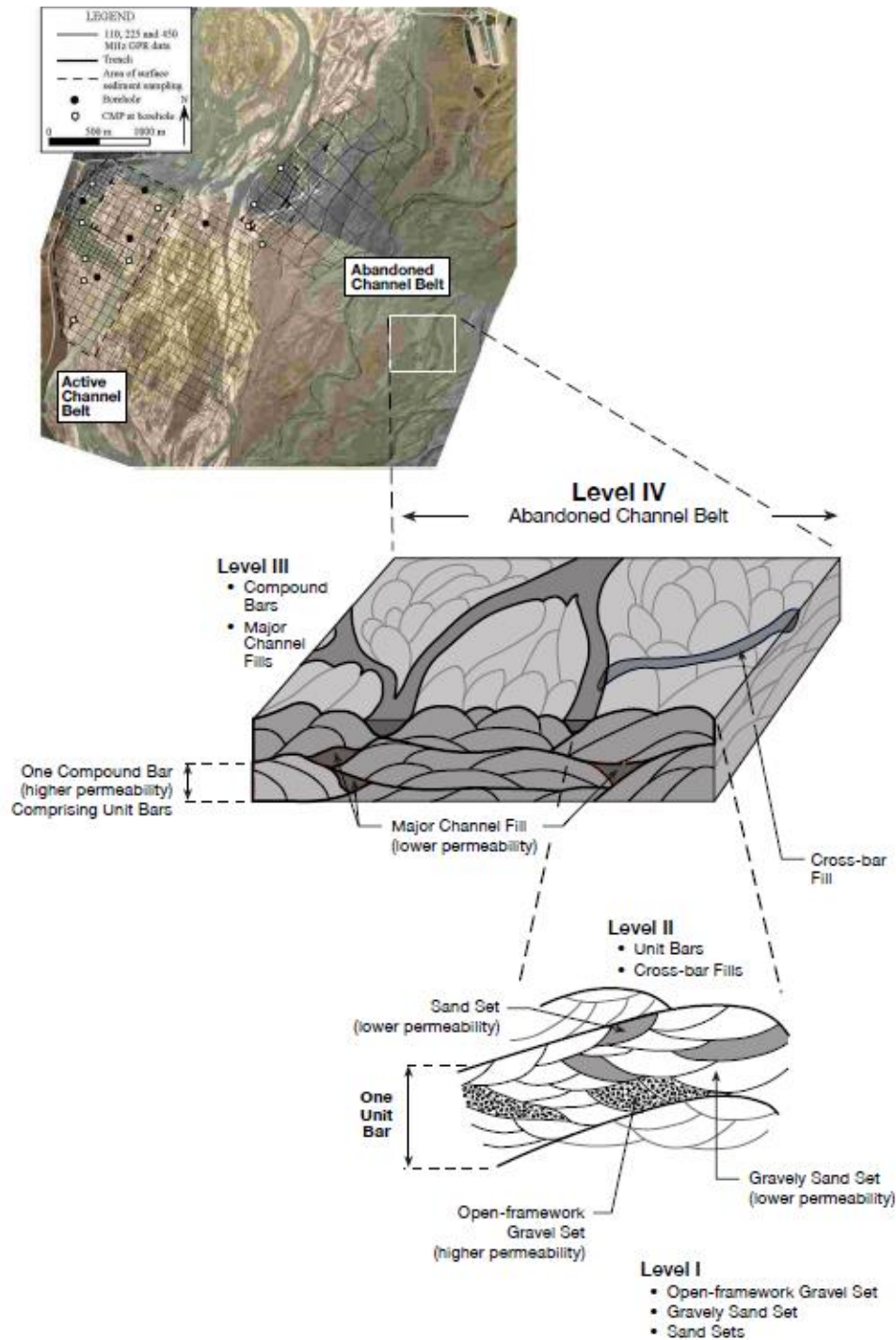


**Figure 1.** (Top) Study areas in the active channel belt and in the preserved channel belt deposits of the Sagavanirktok River (Lunt et al., 2004). (Middle and Bottom) Conceptual model for the hierarchical sedimentary architecture found in channel belt deposits (see also Table 1). The compound bar deposits at level III result from the processes of unit-bar accretion and channel migration. Within unit bar deposits (level II), sets of open-framework gravel (level I) have highest permeability. As channels are abandoned, they are filled with lower-permeability sediment. Major channel fills (level III) and smaller cross-bar channel fills (level II) are lower-permeability baffles within the deposit. From Ramanathan et al. (2010).

Lunt et al. (2004) studied the gravelly channel belt of the Sagavanirktok River (Alaska, Figure 1) and quantified the proportions and lengths for unit types across relevant scales (Table 1). At the smallest scale, sets of cross-stratified (“cross-sets” herein) sand, sandy gravel, and open-framework gravel (decimeters thick and meters long) occur within unit bar deposits (tens of decimeters thick and tens of meters long). Unit bars and cross-bar channel fills occur within compound bar deposits (meters thick and hundreds of meters long). Compound bar deposits and the channel fills that bound them occur within channel belts (tens of meters thick and kilometers long). Importantly, the open-framework gravel cross-sets were found to make up 25 to 30 percent of the volume of the deposit.

Table 1. Hierarchy of Unit Types

IV	channel-belt deposit				
III	compound bar deposits <sup>1</sup>				major channel fills
II	unit bar deposits			cross-bar channel fills	concave-up sand
I	open-framework gravel set <sup>2</sup>	gravelly sand set	sand set	concave-up sand	concave-up sand

<sup>1</sup>. typical dimensions (largest unit type):  $750 \times 500 \times 2 \text{ m}^3$

<sup>2</sup>. typical dimensions (smallest type): decimeters to meters long and wide, centimeters to decimeters thick

The sedimentary architecture quantified by Lunt et al. (2004) was incorporated by Ramanathan et al. (2010) into a high-resolution, three-dimensional, digital model using geometric-based simulation methods. Guin et al. (2010) confirmed that the model contains the hierarchy of sedimentary unit types and honors the proportions, geometries, and spatial distribution of the unit types quantified at each level by Lunt et al. (2004). Figure 2 shows a cross section through an extracted piece of a simulated compound bar deposit sampled with fine resolution (larger scale simulations showing larger-scale architecture are given in Ramanathan et al. (2010, Figure 10).

In this model, cross-sets of high-permeability open-framework gravel (OFG) were simulated discretely. OFG cells are considered to be connected when cell faces are adjacent. Importantly, clusters of continuously connected OFG cells create preferential flow pathways. When OFG cross-sets comprise at least 20% of the volume of the

deposit, clusters span opposing pairs of domain boundaries (Guin et al., 2010). Such spanning, preferential-flow pathways exist as “thief zones” and control miscible gas injection within the Ivishak Formation (Tye et al., 2003).

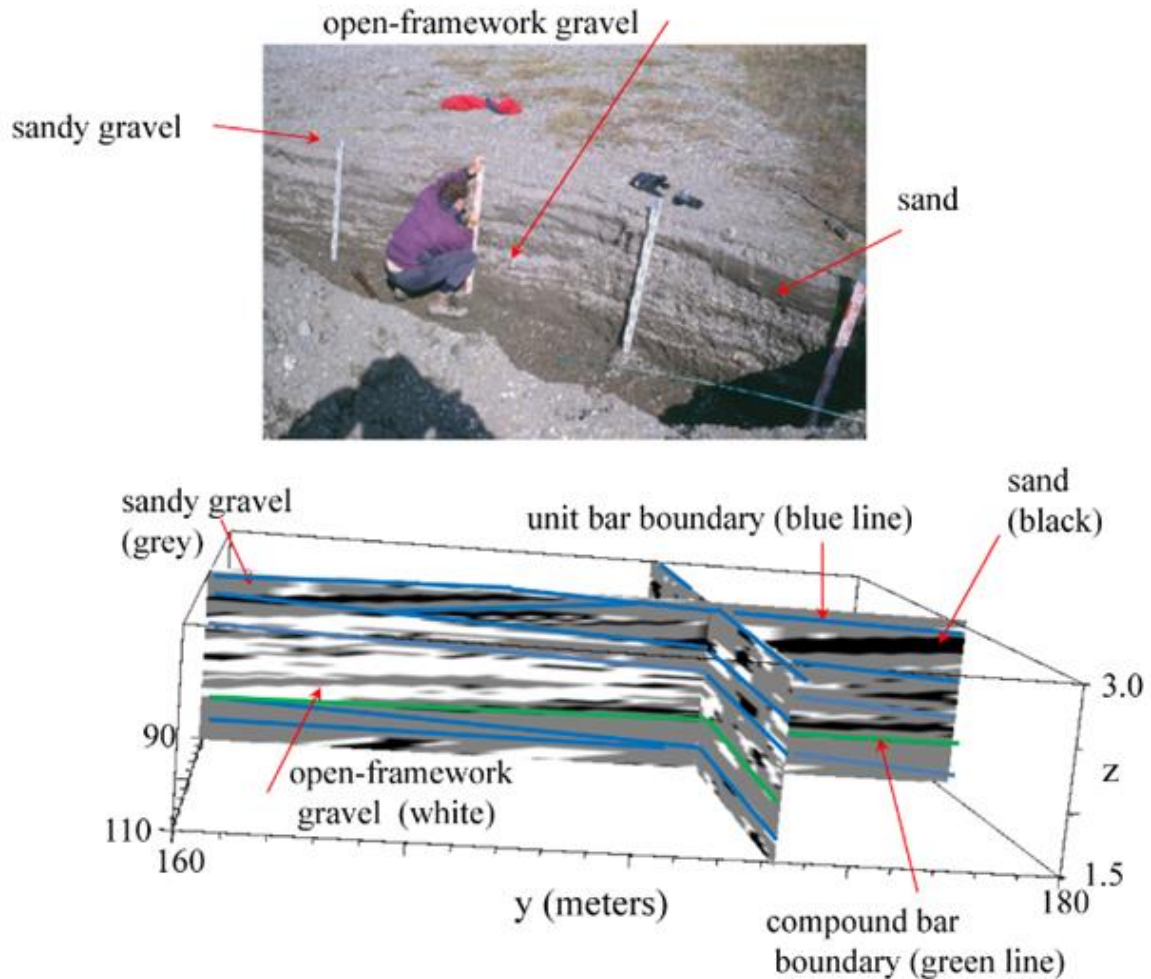


**Figure 2.** (Top) Exposure of level I unit types in a trench at the Sagavanirktok River field site (from Lunt, 2002). (Bottom) Rendering of orthogonal sections through an extracted piece of the stratal model produced for realization 1 with the GEOSIM code. The extracted piece was chosen so that open-framework gravel/conglomerate (28% of overall model volume) was clearly visible. Paleoflow direction is to the left.

The number, size, and orientation of OFG clusters in the model change with proportion. At any given proportion, the number, size, and orientation of clusters changes across the different hierarchical levels (scales) of the stratal architecture. Connected OFG cells within individual cross-sets form paths that vertically span single unit bar deposits. Connections across unit bar boundaries enhance lateral branching and the many clusters

within unit bars connect into a smaller number of larger clusters at the scale of multiple unit bars. At the scale of a whole compound bar deposit, these clusters are typically connected into one or two large, spanning clusters. The spanning clusters occur at proportions of open-framework gravel cells below the theoretical threshold (31%) for random infinite media predicted in the mathematical theory of percolation. Guin and Ritzi (2008) showed that this is caused by geological structure within a finite domain. The percolation theory shows why two-dimensional models under-represent true three-dimensional connectivity, and thus why simulations must be three-dimensional (Huang et al., 2012).

The saturated permeability in sandy-gravel deposits varies non-linearly as a function of the volume of sand mixed with gravel (see Figure 6 in Ramanathan et al., 2010). Sandy-gravel strata have permeabilities similar to the sand they contain, which are of the order of  $10^0$  to  $10^1$  Darcies. Thus, sand and sandy-gravel cross-sets within unit bars have permeabilities similar to channel-fill sands. Open-framework gravels have permeabilities of the order of  $10^3$  to  $10^4$  Darcies. In either type of strata, the coefficient of variation in permeability is of the order of unity. In the lithified stratatypes within the Ivishak Formation (sandstones, pebbly sandstones and open-framework conglomerates), the saturated permeabilities scale down accordingly (Tye et al., 2003).

#### **4. METHODOLOGY**

Using a code by Ramanathan et al. (2010) We generated a realization of the channel-belt architecture including two materials, i.e. sand (76%) and OFG (24%) with geometric mean permeability 58 mD and 3823 mD, respectively. We simulated injection of CO<sub>2</sub> in a reservoir with size 100 m x 100 m x 5 m (250 thousand cells of size 2 m x 2 m x 0.05 m). This represents the heterogeneity created by an assemblage of unit bars within a compound bar. This simulation includes a cluster of OFG cells which tortuously spans the domain boundaries in all directions and contains 55% of all OFG cells. CO<sub>2</sub> was injected at a rate of 3.6 (standard) m<sup>3</sup>/day during 10 days into the bottom of a vertical well at a depth 2360 m. In one case the well was placed to penetrate a spanning OFG cluster and in another case placed so it does not. The boundary of the CO<sub>2</sub> reservoir was

not permeable. For comparison we also simulated injection into two homogeneous reservoirs: (1) homogeneous, isotropic, and with permeability equal to the geometric mean of the heterogeneous reservoir; and (2) homogeneous but anisotropic with permeability five times smaller in the z direction than in horizontal directions.

When simulating CO<sub>2</sub> injection in a reservoir with realistic heterogeneity, the choices for relative permeability and capillary pressure tables are very important. The tables define the relations between water relative permeability, CO<sub>2</sub> relative permeability, and CO<sub>2</sub> capillary pressure as a function of water saturation. Two different sets of tables were utilized for the sand and OFG unit types. Thus, the total number of property tables was 12 including six for drainage and six for imbibition.

To generate tables we used the following methodology. First we find the irreducible water saturation and the maximum CO<sub>2</sub> saturation, adapting the approach described by Holtz (2002). Using an empirical relation between permeability ( $k$ ) and porosity  $\phi$ , we obtain porosity for sand and OFG (see Table 2).

$$k = 7 \cdot 10^7 \phi^{9.61}. \quad (1)$$

Then from the following empirical relation (Holtz, 2002) we find the averaged irreducible water saturation ( $S_{wi}$ ) for both materials (Table 2).

$$S_{wi} = 5.159(\log(k)/\phi)^{-1.559} \quad (2)$$

Residual CO<sub>2</sub> saturation ( $S_{gr}$ ) can be found from the following empirical relation (Holtz, 2002):

$$S_{gr} = -0.969\phi + 0.5473 . \quad (3)$$

The next step is calculation of capillary pressure for drainage ( $P_{cd}$ ) using the Brooks-Corey relation (Brook and Corry, 1964):

$$P_c = P_e \left( \frac{S - S_{wi}}{1 - S_{wi}} \right)^{-1/\lambda}, \quad (4)$$

where  $S$  is water saturation,  $P_e$  is the minimum pressure required for the entry of CO<sub>2</sub> into the pore of the rock and  $\lambda$  is a fitting parameter known as pore size distribution index. For rocks from the Mt. Simon Formation  $P_e = 4.6 \cdot 10^3 \text{ Pa}$  and  $\lambda = 0.55$  (Krevor et al., 2012). We use this value for the sand. To find the entry pressure point for OFG we scale the sand value based on the Leverett  $J$ -function as Saadatpoor et al. (2009) proposed:

$$P_e^{OFG} = P_e \left( \frac{k_{sand} \phi_{OFG}}{k_{OFG} \phi_{sand}} \right)^{0.5}.$$

For imbibition we use a curve analogous to (4) but, in contrast to drainage, the imbibition curve cross the saturation axis at value  $S = 1 - S_{gr}$ .

For the relative permeability curves the Brooks-Corey relations in the form proposed by Dullien (1992) are used:

$$k_{r,w} = (S_w^*)^{N_w} \quad (5)$$

$$k_{r,CO_2} = k_{r,CO_2}(S_{wi})(1 - S_w^*)^2 [1 - (S_w^*)^{N_{CO_2}}], \quad (6)$$

where  $S_w^* = \frac{S - S_{wi}}{1 - S_{wi}}$  for (5) and  $S_w^* = \frac{S - S_{wi}}{1 - S_{gr} - S_{wi}}$  for (6). The variables  $N_w$  and  $N_{CO_2}$  are used as fitting parameters known as the Corey exponents for water and CO<sub>2</sub>, respectively. The following values are used:  $N_{CO_2} = 4$  (Krevor et al., 2012),  $N_w = 5$  and  $N_w = 3$  for drainage and imbibition. The values of other parameters are in the Table 2.

Table 2

	$\phi$	$S_{wi}$	$S_{gr}$	$k_{r,CO_2}(S_{wi})$	$P_e$ (Pa)
sand	0.23	0.22	0.32	0.65	$4.6 \cdot 10^3$
OFG	0.36	0.1426	0.2	0.95	$0.72 \cdot 10^3$

The results are summarized in Figure 3.

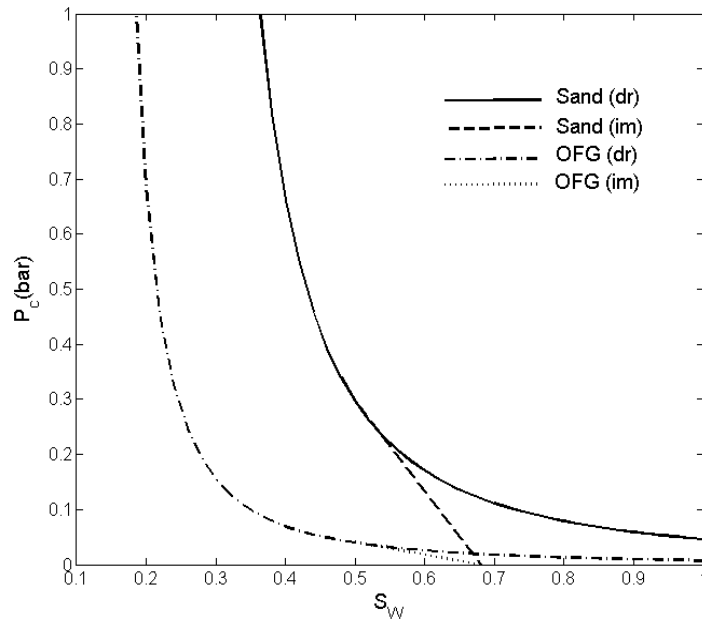


Figure 3a. Capillary pressure for sand and OFG for drainage and imbibition.

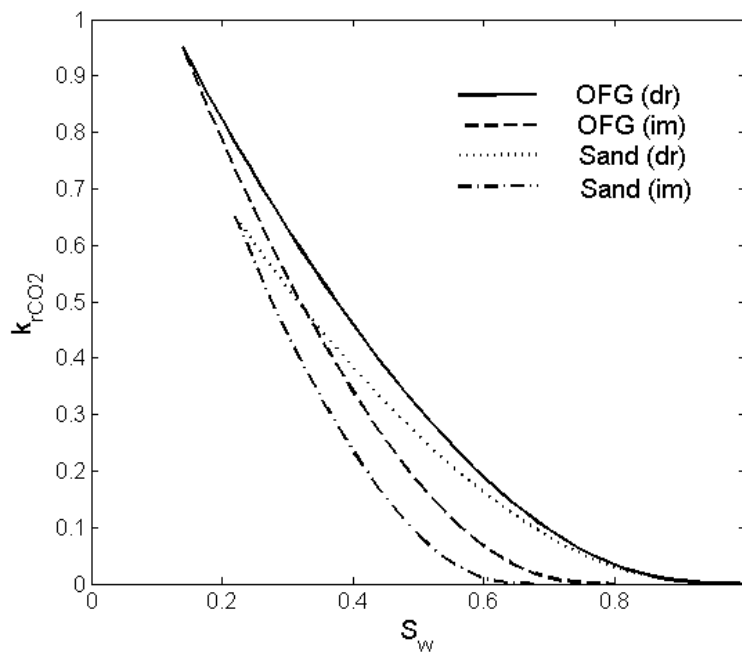


Figure 3b. Relative permeability of CO2 in sand and OFG for drainage and imbibition.

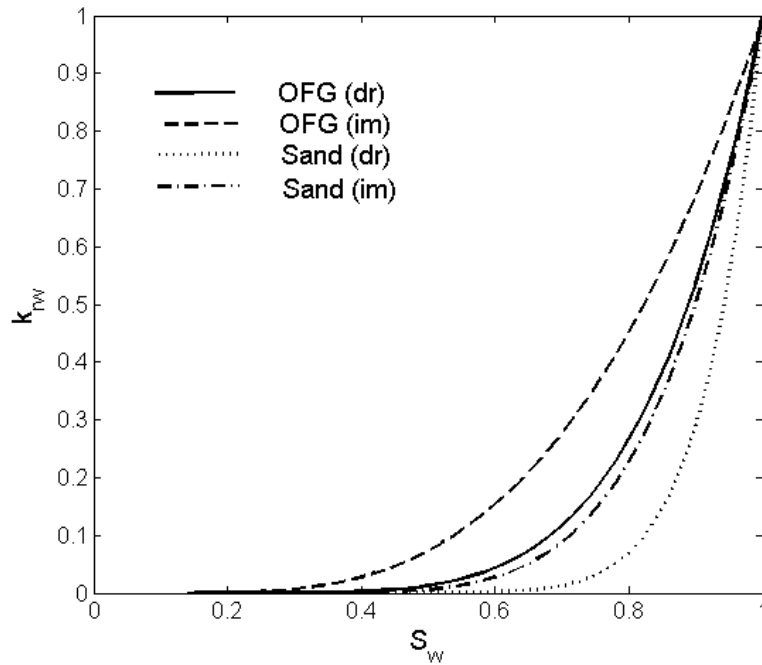


Figure 3c. Relative permeability of water in sand and OFG for drainage and imbibition.

## 5. RESULTS AND DISCUSSION

Figures 4 and 5 shows vertical cross sections with CO<sub>2</sub> saturation for the heterogeneous and homogeneous anisotropic reservoirs after 10 days and after 1010 days, respectively. After injection CO<sub>2</sub> propagates in the horizontal and vertical directions. The force of buoyancy moves the CO<sub>2</sub> plume up.

The ratio of the viscous to gravity forces defines the geometry of the plume in the homogeneous case. In the homogeneous anisotropic reservoir the CO<sub>2</sub> plume reaches the top of the reservoir in 10 days and then the top of the plume slowly spreads laterally. Essentially the same behaviour is exhibited by a plume in the homogeneous isotropic reservoir (not shown), but in the latter the plume reaches the top of the reservoir 5 times faster (in 2.5 days). The shape of the plume, the rate of capillary trapping of CO<sub>2</sub>, and the CO<sub>2</sub> solution in brine are similar in these two cases.

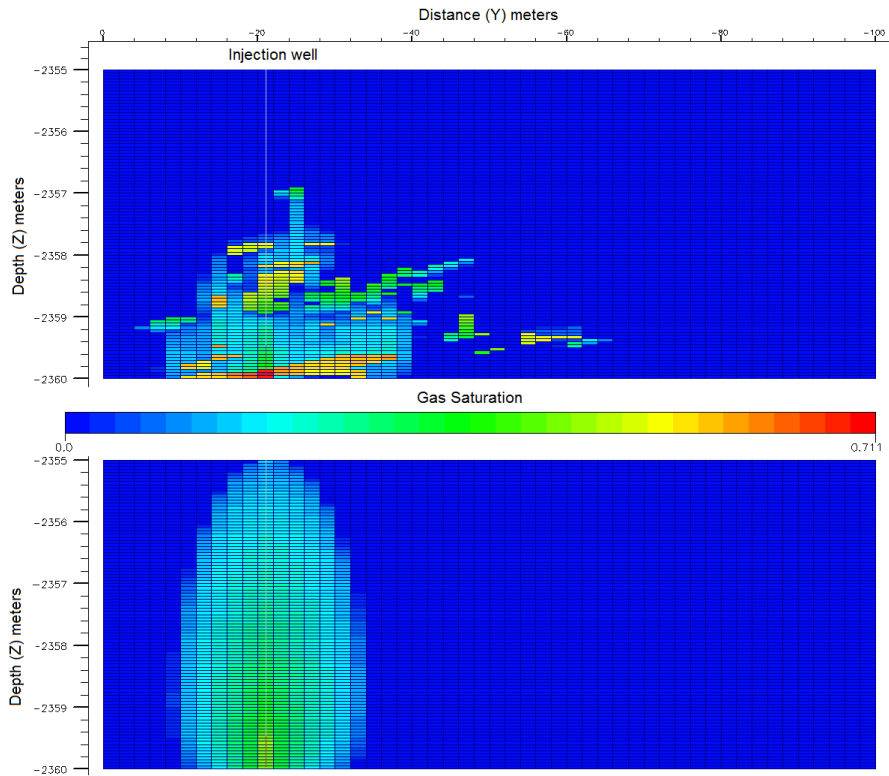


Figure 4. Vertical cross section of heterogeneous (top) and homogeneous anisotropic (bottom) reservoirs showing CO<sub>2</sub> saturation after 10 days from the beginning of CO<sub>2</sub> injection.

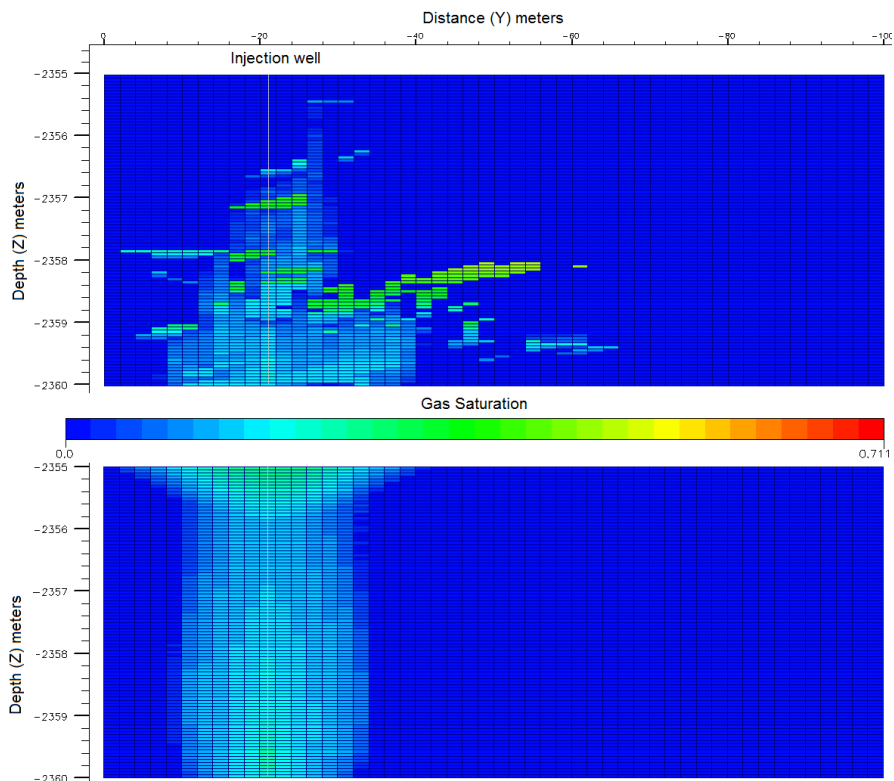


Figure 5. Vertical cross section of heterogeneous (top) and homogeneous (bottom) reservoirs showing CO<sub>2</sub> saturation after 270 days from the beginning of CO<sub>2</sub> injection.

In contrast, in the heterogeneous case the plume is two times wider and never reaches the top of the reservoir (see Figure 5, top panels). This is caused by the difference in capillary entry pressure between sand and OFG and the presence of multiple boundaries between sand and OFG. After injection a buoyancy force moves the CO<sub>2</sub> plume up. In the heterogeneous case it is more complicated. CO<sub>2</sub> propagates faster in OFG clusters since permeability of OFG material is much higher than in sand. However, in clusters that do not span the domain, CO<sub>2</sub> cannot escape from the cluster and remains trapped unless the buoyancy force is large enough to overcome the capillary entry pressure of sand. In spanning clusters, CO<sub>2</sub> propagates mainly in the horizontal direction since OFG clusters extend further in this direction. CO<sub>2</sub> can exit from a spanning OFG cluster through its upper boundary if buoyancy force is large enough. It will propagate upward through sand to the next OFG cluster, into which it will be pushed by both buoyancy force and capillary pressure. This process continues up to the point when buoyancy force becomes comparable with capillary pressure and the plume becomes immobile or trapped, or the plume reaches the top of the reservoir.

Due to the process described above the contact area between brine and the CO<sub>2</sub> plume is larger than in the homogeneous case. As a result the dissolution rate is larger in the heterogeneous case. The “regular” capillary trapping rate is also largely affected. Overall the results indicate that the presence of small and large OFG clusters essentially controls behavior of CO<sub>2</sub> plumes on reservoir scale.

Importantly, in the heterogeneous case considered here the plume never reaches the caprock. Total amount of inserted CO<sub>2</sub> is effectively trapped. The trapping is mostly in sand (in blobs and ganglia) and by the secondary sealing effect in OFG material (on the boundary between sand and OFG).

Injected CO<sub>2</sub> can be apparently divided into four parts, i.e. 1) mobile gas, 2) immobile gas trapped in the form of blobs and ganglia by hysteresis, 3) gas trapped at the boundary between sand and OFG due to different entry point pressures, and 4) dissolved gas. Note that gas trapped at the boundary between sand and OFG could be mobilized by increased gas injection, pushing it through the boundary.

Figure 6 depicts the total amount of the mobile, capillary trapped, and solute CO<sub>2</sub> in sand and OFG. While OFG material comprises only 24% of the reservoir, most of the mobile CO<sub>2</sub> is in OFG cells. (Figure 6a). The amount of capillary trapped CO<sub>2</sub> in OFG is about twice that in sand (Figure 6b). The amount of solute CO<sub>2</sub> is two to three times larger in sand than in OFG (Figure 6c).

To further illustrate the roles of 1) capillary pressure, 2) hysteresis of relative permeability of water and CO<sub>2</sub> and 3) heterogeneity of permeability on plume geometry and dynamics as well as on CO<sub>2</sub> trapping and dissolution we compare the results of the five cases described in Table 3.

The results from each case are given in Figure 7. Case 1 includes heterogeneity and all 12 property tables; it is the standard for comparison. This figure shows that plume geometry is very different from case to case. The plume quickly reaches the top of the reservoir for the homogeneous reservoir (case 2), in heterogeneous reservoir with capillary pressure “off” (case 5) and if capillary pressure is “on” but the properties tables are the same for both materials (case 3). In contrast, the spreading of the plume in the vertical direction is much slower in cases 1 and 4. The results illustrate that the most important factor affecting capillary trapping is the different entry point pressures for the different geologic unit types (the so called secondary seal effect).

**Table 3**

Case #	Permeability	Capillary pressure	Hysteresis	Relative Permeability tables	Number of tables
1	Heterogeneous	on	on	Different for sand and OFG	12
2	Homogeneous, Anisotropic	on	on	The same for all cells	6
3	Heterogeneous	on	on	The same for all cells	6
4	Heterogeneous	on	off	Different for sand and OFG	6
5	Heterogeneous	off	on	Different for sand and OFG	6

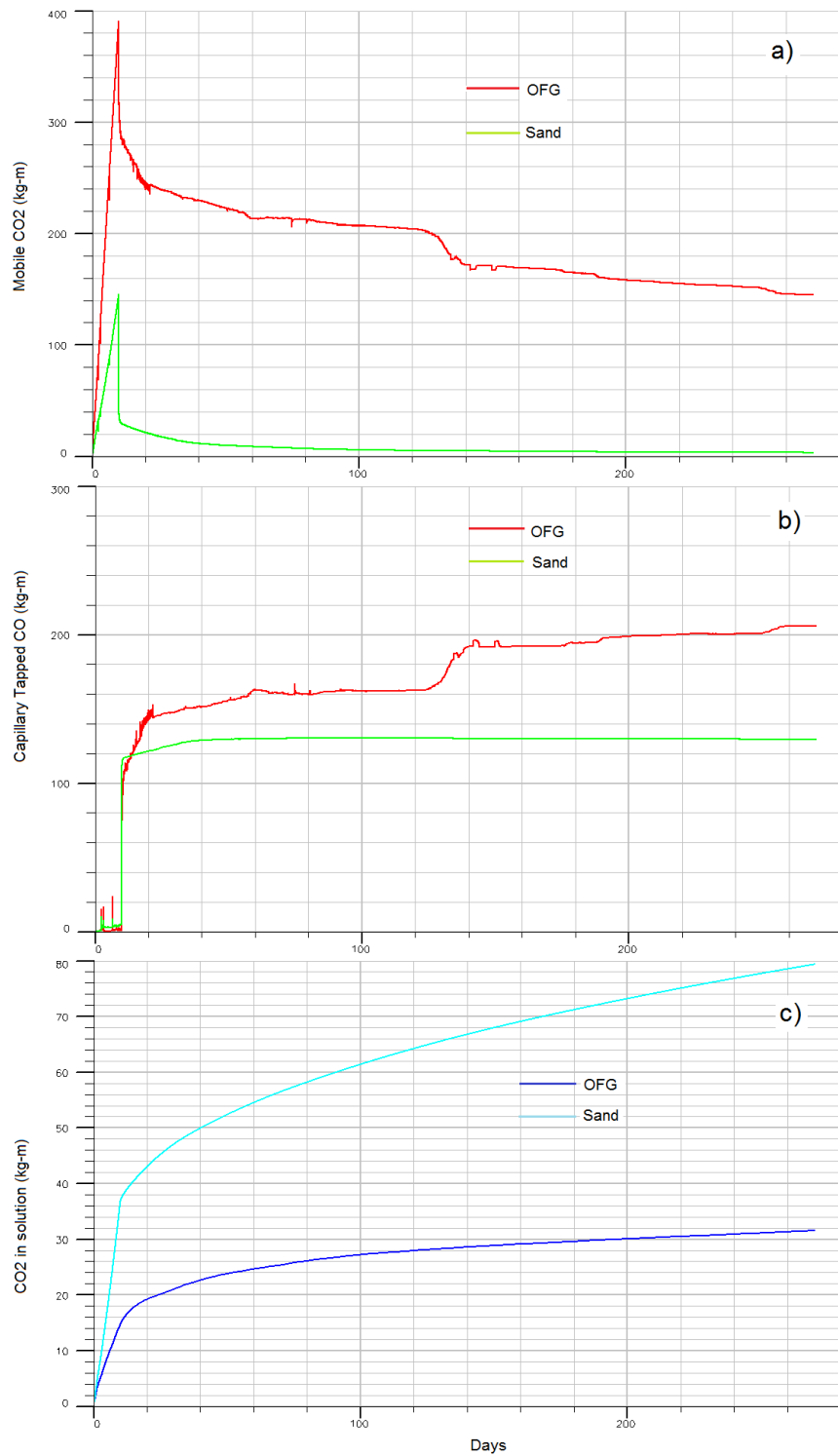


Figure 6. Total amount of the mobile (a), capillary trapped (b), and solute CO<sub>2</sub> (c) in sand and OFG as function of time.

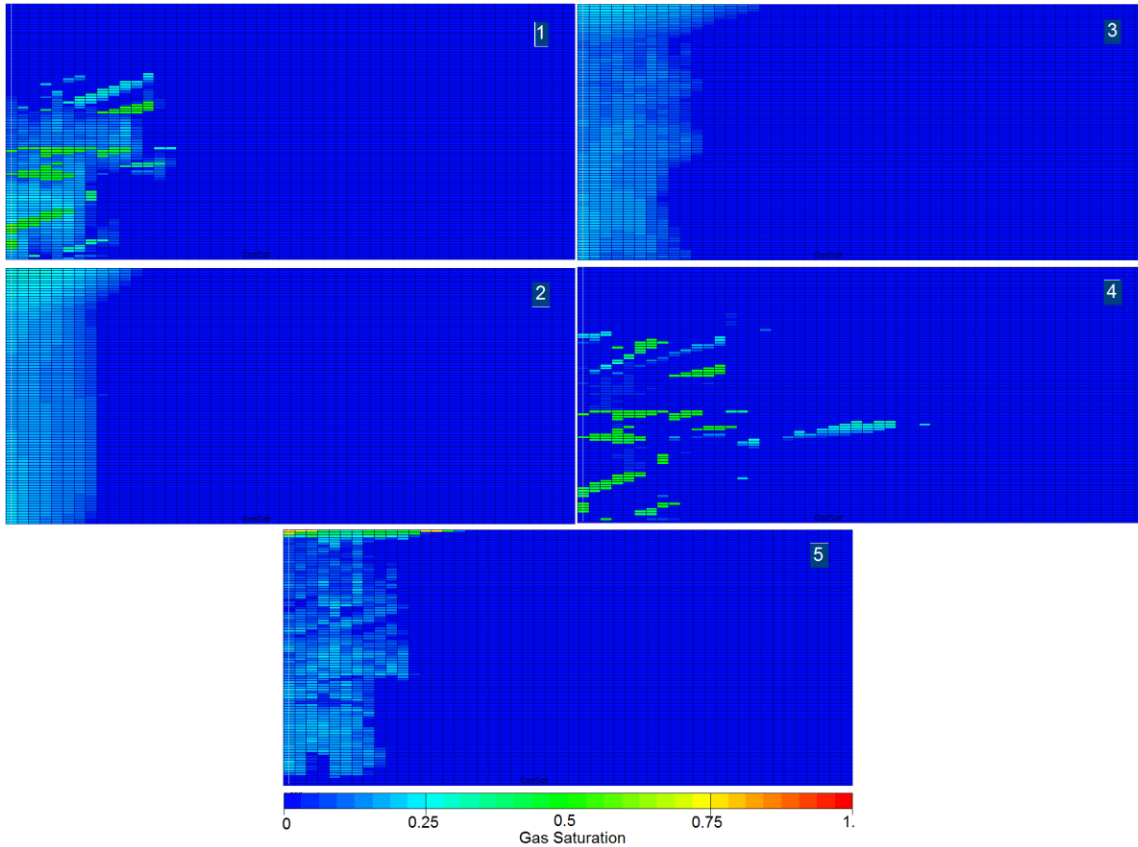


Figure 7. Vertical cross section of reservoirs showing CO2 saturation after 170 days from the beginning of CO2 injection for the five cases described in the Table 3. Well placed at a depth 2360 m.

## 6. CONCLUSIONS

Several features distinguish our approach from others:

1) The modeled heterogeneity structure and scales, hence permeability map, realistically reflects the typical fluvial type reservoirs; permeability ranges by 4 orders of magnitude.

2) The size of reservoir heterogeneities ranges from a few cm to dozens of meters.

3) The reservoir contains two different materials -- sand and open framework gravel -- with different properties, requiring that two sets of property tables be used for simulation.

4) Capillary pressure and hysteresis effects are utilized in the simulation. Overall, 12 properties tables were used including relative permeability and capillary pressure curves for drainage and imbibition for both brine and CO2.

The results demonstrate that small and medium scale inclusions of high-permeability cross strata fundamentally control trapping processes and hence the shape and dynamics of the CO<sub>2</sub> plume. This occurs because the capillary entry pressures of the two materials are different. In a highly heterogeneous reservoir this trapping mechanism may considerably surpass all other capillary trapping mechanisms. Indeed, in the example considered here (Figure 2b) the total amount of injected CO<sub>2</sub> is trapped and never reaches the top of the reservoir. The results strongly suggest that representing these small-scale features, and representing how they are organized within a hierarchy of larger-scale features, is critical to understanding trapping processes. It is also obvious that ignoring both the small-scale heterogeneity and the secondary-seal effect in simulations of CO<sub>2</sub> sequestration may produce misleading results.

A number of studies have considered CO<sub>2</sub> sequestration in fluvial reservoirs but have not represented sedimentary architecture at the scale of our study (e.g. Zhou et al., 2009; Delshad, et al, 2013). The results of our study indicate that the amount of trapping of CO<sub>2</sub> and the geometry of the CO<sub>2</sub> plume may be very different from the results of their current simulations if sedimentary architecture is represented at smaller scales.

The total amount of trapped (immobile) gas and its spatial distribution are different in heterogeneous and homogeneous cases with similar averaged characteristics. It is interesting that the mobile part of the gas is placed mostly inside of high-permeability material, i.e. OFG. The ratio between amounts of gas in OFG to sand is about 8, although reservoir contains only 24% of OFG material. At the same time the amount of capillary trapped immobile gas is larger in sand.

Plume dynamics and the amount of trapped CO<sub>2</sub> depend on the structure and content of the OFG cross strata, and how these are organized within larger units. The large OFG clusters and especially spanning clusters are responsible for the horizontal extent of CO<sub>2</sub> plume, which may three times larger than in the case of a homogeneous reservoir. The size and shape of clusters are important with respect to the amount of gas trapped.

The simulations presented here were performed using a relatively small piece of the geologic model and with injection of small amount of CO<sub>2</sub>. We expect that simulations representing larger scales of the stratal architecture will be important to further

understanding trapping in the reservoir. It is also important to study how the amount, rate, and schedule of CO<sub>2</sub> injection affect trapping processes.

## ACKNOWLEDGMENTS

We thank Schlumberger Limited for the donation of ECLIPSE Reservoir Simulation Software and the Ohio Supercomputer Center for technical support.

## REFERENCES

- Altundas, Y.B., T.S. Ramakrishnan, N. Chugunov and R. de Loubens (2011), Retardation of CO<sub>2</sub> Caused by Capillary Pressure Hysteresis: A New CO<sub>2</sub> Trapping Mechanism, *SPE Journal*, 16 (4), 784-794.
- Ambrose, W. A., S. Lakshminaraashimah, M. H. Holtz, N. Nunez - Lopez, S. D. Hovorka, and I. Duncan (2008), Geologic factors controlling CO<sub>2</sub> storage capacity and permanence: Case studies based on experience with heterogeneity in oil and gas reservoir applied CO<sub>2</sub> storage, *Environ. Geol.*, 54, 1619–1633.
- Bachu, S. (2000), Sequestration of CO<sub>2</sub> in geological media: Criteria and approach for site selection in response to climate change, *Energy Convers. Management*, 41(9), 953–970.
- Bachu, S. (2003), Sequestration of CO<sub>2</sub> in geological media in response to climate change: Capacity of deep saline aquifers to sequester CO<sub>2</sub> in solution, *Energy Convers. Management*, 44(20), 3151– 3175.
- Bridge, J.S. (2006), Fluvial facies models: Recent developments, in *Facies Models Revisited*, SEPM Spec. Publ., 84, edited by H. W. Posamentier and R. G. Walker, pp. 85–170, Soc. for Sediment. Geol. (SEPM), Tulsa, Okla.
- Brooks, R. J., and A. T. Corey (1964), Hydraulic properties of porous media, *Hydrol. Pap.* 3, Colo. State Univ., Fort Collins
- Bruant, R. G., Jr., M. A. Celia, A. J. Guswa, and C. A. Peters (2002), Safe storage of CO<sub>2</sub> in deep saline aquifers, *Environ. Sci. Technol.*, 36(11), 240A– 245A.
- Bryant, S. L., S. Lakshiminarasimhan, and G. A. Pope (2006), Buoyancy-dominated multiphase flow and its impact on geological sequestration of CO<sub>2</sub>, SPE 99938, SPE/DOE Symposium on Improved Oil Recovery, Tulsa, Okla.

Burton, M., N. Kumar and S.L. Bryant (2009), CO<sub>2</sub> injectivity into brine aquifers: why relative permeability matters as much as absolute permeability, *Energy Procedia* 1, 3091–3098

Dai Z, Middleton R, Viswanathan H, Fessenden-Rahn J, Bauman J, Pawar R, B. McPherson (2013), An integrated framework for optimizing CO<sub>2</sub> sequestration and enhanced oil recovery, *Environmental Science & Technology Letters*,1(1), 49-54

Delshad, M., X. Kong, R. Tavakoli, S.A. Hosseini, and M.F. Wheeler (2013), Modeling and simulation of carbon sequestration at Cranfield incorporating new physical models. *Int. J. Greenhouse Gas Control*, 18, 463–473

Deng H, Stauffer P H, Dai Z, Jiao Z, Surdam R C (2012), Simulation of industrial-scale CO<sub>2</sub> storage: Multi-scale heterogeneity and its impacts on storage capacity, injectivity and leakage, *Int. J. Greenhouse Gas Control*, 2012, 10, 397-418.

Doughty, C. and K. Pruess. (2004), Modeling supercritical CO<sub>2</sub> injection in heterogeneous porous media. *Proceeding, TOUGH Symposium 2003*, Lawrence Berkeley National Laboratory, Berkeley, California, May 12–14.

Dullien, F.A.L. (1992), *Porous Media Fluid Transport and Pore Structure*, Academic, San Diego.

Ennis-King, J., and L. Paterson (2005), Role of convective mixing in the long-term storage of carbon dioxide in deep saline formations, *Soc. Pet. Eng. J.*, 10(3), 349– 356.

Forster, A., et al. (2006), Base characterization of the CO<sub>2</sub>SINK geological storage site at Ketzin, Germany, *Environ. Geosci.*, 13, 145–161.

Flett, M., R. Gurton, and G. Weir (2007), Heterogeneous saline formations for carbon dioxide disposal: Impact of varying heterogeneity on containment and trapping, *J. Pet. Sci. Eng.*, 57, 106–118.

Gershenson, N. I., M. Soltanian, R.W. Ritzi Jr, & D. F. Dominic (2014), Understanding the impact of open-framework conglomerates on water-oil displacements: Victor interval of the Ivishak reservoir, Prudhoe Bay Field, Alaska. *arXiv preprint arXiv:1405.3998*.

Gershenson, N. I., M. Soltanian, R.W. Ritzi Jr, & D. F. Dominic (2014), CO<sub>2</sub> capillary-trapping processes in deep saline aquifers. *Geophysical Research Abstracts*, 2014, 16, EGU2014-3935.

Guin, A., & R. W. Ritzi Jr. (2008), Studying the effect of correlation and finite-domain size on spatial continuity of permeable sediments. *Geophys. Res. Lett.*, 35 (10), L10402, doi:10.1029/2007GL032717

Guin, A., R. Ramanathan, R.W. Ritzi Jr., D.F. Dominic, I.A. Lunt, T.D. Scheibe, and V.L. Freedman (2010), Simulating the heterogeneity in braided channel belt deposits: 2.

Examples of results and comparison to natural deposits, *Water Resour. Res.*, 46, W04516, doi:10.1029/2009WR008112.

Han, W. S., S. - Y. Lee, C. Lu, and B. J. McPherson (2010), Effects of permeability on CO<sub>2</sub> trapping mechanisms and buoyancy - driven CO<sub>2</sub> migration in saline formations, *Water Resour. Res.*, 46, W07510, doi:10.1029/2009WR007850

Hesse M.A., H.A. Tchelepi, B.J. Cantwell and F.M. Orr Jr. (2007), Gravity currents in horizontal porous layers: transition from early to late self-similarity. *J. Fluid Mech.* 577, 363–383

Hitchon, G., W. D. Gunter, T. Gentzis, and R. T. Bailey (1999), Sedimentary basins and greenhouse gases: A serendipitous association, *Energy Convers. Management*, 40(8), 825– 843.

Holloway, S. (2001), Storage of fossil fuel-derived carbon dioxide beneath the surface of the earth, *Annu. Rev. Energy Environ.*, 26, 145– 166.

Holtz, M.H. (2002), Residual Gas Saturation to Aquifer Influx: A Calculation Method for 3-D Computer Reservoir Model Construction, paper was prepared for presentation at the SPE Gas Technology Symposium held in Calgary, Alberta, Canada, 30 April–2 May 2002.

Hovorka S.D., C. Doughty, S. M. Benson, K. Pruess and P.R. Knox (2004), The impact of geological heterogeneity on CO<sub>2</sub> storage in brine formations: a case study from the Texas Gulf Coast. Geological Society, London, Special Publications, 233, 147-163.

Huang, L., Ritzi, R. W., & Ramanathan, R. (2012), Conservative models: Parametric entropy vs. temporal entropy in outcomes. *Groundwater*, 50(2), 199-206.

Hunt, J. R., N. Sitar, and K. S. Udell (1988), Nonaqueous phase liquid transport and cleanup: 1. Analysis of mechanisms, *Water Resour. Res.*, 24(8), 1247–1258.

Ide, S.T., K. Jessen, F.M. Orr Jr. (2007), Storage of CO<sub>2</sub> in saline aquifers: Effects of gravity, viscous, and capillary forces on amount and timing of trapping, *international journal of greenhouse gas control* 1, 481 – 491.

Intergovernmental Panel on Climate Change (2007), *Climate change 2007: Mitigation of Clim. Change: Working Group III Contribution to the Fourth Assessment Report of the Intergovernmental Panel on Clim. Change*, Cambridge University Press, Cambridge.

Juanes, R., E. J. Spiteri, F. M. Orr Jr., and M. J. Blunt (2006), Impact of relative permeability hysteresis on geological CO<sub>2</sub> storage, *Water Resour. Res.*, 42, W12418, doi:10.1029/2005WR004806

Kovscek, A. R., and M. D. Cakici (2005), Geologic storage of carbon dioxide and enhanced oil recovery. II. Cooptimization of storage and recovery, *Energy Convers. Manage.*, 46, 1941– 1956.

Kovscek, A. R., and Y. Wang (2005), Geologic storage of carbon dioxide and enhanced oil recovery. I. Uncertainty quantification employing a streamline based proxy for reservoir flow simulation, *Energy Convers. Management*, 46, 1920– 1940.

Krevor, S. C. M., R. Pini, L. Zuo, and S. M. Benson (2012), Relative permeability and trapping of CO<sub>2</sub> and water in sandstone rocks at reservoir conditions, *Water Resour. Res.*, 48, W02532, doi:10.1029/2011WR010859.

Kuo C W, Benson S. (2013), Analytical Study of Effects of Flow Rate, Capillarity and Gravity on CO<sub>2</sub>/Brine Multiphase Flow System in Horizontal Corefloods. *SPE Journal*, 18(4), 708-720.

Kumar, A., R. Ozah, M. Noh, G. A. Pope, S. Bryant, K. Sepehrnoori, and L. W. Lake (2005), Reservoir simulation of CO<sub>2</sub> storage in deep saline aquifers, *Soc. Pet. Eng. J.*, 10(3), 336– 348.

Leonenko Y. and D.W. Keith (2008), Reservoir engineering to accelerate the dissolution of CO<sub>2</sub> stored in aquifers. *Environ. Sci. Technol.* 42, 2742–2747.

Lindeberg, E. and D. Wessel-Berg (1997), Vertical convection in an aquifer column under a gas cap of CO<sub>2</sub>. *Energy Convers. Manage.* 38, S229–S234, doi:10.1016/S0196-8904(96)00274-9

Lunt, I.A. (2002), A three-dimensional, quantitative depositional model of gravelly braided river sediments with special reference to the spatial distribution of porosity and permeability, Phd dissertation, Binghamton University, State University of New York.

Lunt, I.A., J.S. Bridge, and R.S. Tye (2004), A quantitative, three dimensional depositional model of gravelly braided rivers, *Sedimentology*, 51(3), 377–414, doi:10.1111/j.1365-3091.2004.00627.x.

Lunt, I.A. and J.S. Bridge (2007) Formation and preservation of open framework gravel strata in unidirectional flows, *Sedimentology*, 54, 71–87, doi:10.1111/j.1365-3091.2006.00829.x.

McGuire, P.L., R.S. Redman, W.L. Mathews, and S.R. Carhart (1999), Unconventional miscible EOR Experience at Prudhoe Bay: *Journal of Petroleum Technology*, 51(1), 38–41.

Middleton, R.S., G.N. Keating, P.H. Stauffer, A.B. Jordan, H.S. Viswanathan, Q.J. Kang, J.W. Carey, M.L. Mulkey, E.J. Sullivan, S.P. Chu, R. Esposito and T.A. Meckel (2012),

The cross-scale science of CO<sub>2</sub> capture and storage: from pore scale to regional scale  
*Energy Environ. Sci.*, 5, 7328-7345 DOI: 10.1039/C2EE03227A

Mo, S., P. Zweigel, E. Lindeberg, and I. Akervoll (2005), Effect of geologic parameters on CO<sub>2</sub> storage in deep saline aquifer, SPE 93952 presented at 14th Europec Biennial Conference, Madrid, Spain.

Mo, S. and Akervoll, I., (2005), Modelling Long-Term CO<sub>2</sub> Storage in Aquifer with a Black-Oil Reservoir Simulator, Paper SPE93951, Presented at the 2005 SPE/EPA/DOE Exploration and Production Environmental Conference, Texas, U.S.A.

Obi, E.-O. I., and M. J. Blunt (2006), Streamline-based simulation of carbon dioxide storage in a North Sea aquifer, *Water Resour. Res.*, 42, W03414, doi:10.1029/2004WR003347.

Pruess, K., and J. Garcí'a (2002), Multiphase flow dynamics during CO<sub>2</sub> disposal into saline aquifers, *Environ. Geol.*, 42(2–3), 282– 295.

Qi, R., T.C. LaForce, and M.J. Blunt (2009) Design of carbon dioxide storage in aquifers, *International Journal of Greenhouse Gas Control*, 3, 195 – 205.

Ramanathan, R., A. Guin, R.W. Ritzi, D.F. Dominic, V.L. Freedman, T.D. Scheibe, and I.A. Lunt (2010), Simulating the heterogeneity in channel belt deposits: Part 1. A geometric-based methodology and code, *Water Resources Research*, v. 46, W04515. DOI:10.1029/2009WR008111.

Ritzi R.W. (2013), *Geometric Simulation of Hierarchical Stratal Architecture: Channel-Belt model (Software Manual & Methods)*. Department of Earth and Environmental Sciences, Wright State University.

Saadatpoor, E., Steven L. Bryant, K. Sepehrnoori (2009), Effect of capillary heterogeneity on buoyant plumes: A new local trapping mechanism *Energy Procedia*, 1(1), 3299–3306

Sakaki, T., M. R. Plampin, R. Pawar, M. Komatsu, T. H. Illangasekare (2013) What controls carbon dioxide gas phase evolution in the subsurface? Experimental observations in a 4.5 m-long column under different heterogeneity conditions: *International Journal of Greenhouse Gas Control* 17 (2013) 66–77; DOI: 10.1016/j.ijggc.2013.03.025

Shamshiri, H., and B. Jafarpour (2012), Controlled CO<sub>2</sub> injection into heterogeneous geologic formations for improved solubility and residual trapping, *Water Resour. Res.*, 48, W02530, doi:10.1029/2011WR010455.

Spiteri, E. J., R. Juanes, M. J. Blunt, and F. M. Orr (2008), A new model of trapping and relative permeability hysteresis for all wettability characteristics, *SPE J.*, 13(3), 277–288.

Steinberg, M. (1992), History of CO<sub>2</sub> greenhouse gas mitigation technologies. *Energy Conversion and Management* 33 (5–8), 311–315

Tye, R. S., B. A. Watson, P. L. McGuire, and M. M. Maguire (2003), Unique horizontal-well designs boost primary and EOR production, Prudhoe Bay field, Alaska, in T. R. Carr, E. P. Mason, and C. T. Feazel, eds., *Horizontal wells: Focus on the reservoir: AAPG Methods in Exploration* 14, 113–125

Tsang, C. - F., J. Birkholzer, and J. Rutqvist (2008), A comparative review of hydrologic issues involved in geologic storage of CO<sub>2</sub> and injection disposal of liquid waste, *Environ. Geol.*, 54, 1723–1737.

Xu, T., J.A. Apps and K. Pruess (2003), Reactive geochemical transport simulation to study mineral trapping for CO<sub>2</sub> disposal in deep saline arenaceous aquifers. *J. Geophys. Res.*108 (B2), 2071.

Zhou, D., Fayers, F.J., Orr, F.M., Jr., 1994. Scaling Multiphase Flow in Simple Heterogeneous Porous Media, SPE 27833, presented at SPE/DOE Ninth Symposium on Enhanced Oil Recovery, Tulsa, April 17–20.

Zhou, Q., J.T. Birkholzer, E. Mehnert, Y-F. Lin, and K. Zhang (2009), Modeling Basin- and Plume-Scale Processes of CO<sub>2</sub> Storage for Full-Scale Deployment, *Ground Water*. 48(4), 494-514. doi: 10.1111/j.1745-6584.2009.00657.x. Epub 2009 Dec 15